Journal of Zhejiang University-SCIENCE B (Biomedicine & Biotechnology)
ISSN 1673-1581 (Print); ISSN 1862-1783 (Online)
www.jzus.zju.edu.cn; www.springerlink.com
E-mail: jzus@zju.edu.cn

Cellular stress and redox activity proteins are involved in gastric carcinogenesis associated with *Helicobacter pylori* infection expressing high levels of thioredoxin-1*#

Yan-yan SHI[1], Jing ZHANG[2], Ting ZHANG[3], Man ZHOU[4], Ye WANG[2], He-jun ZHANG[2], Shi-gang DING†‡[2]

[1]*Research Center of Clinical Epidemiology, Peking University Third Hospital, Beijing 100191, China*
[2]*Department of Gastroenterology, Peking University Third Hospital, Beijing 100191, China*
[3]*Department of Microbiology, Peking University Health Science Center, Beijing 100191, China*
[4]*Department of Biomedical Engineering, College of Engineering, Peking University, Beijing 100871, China*
†E-mail: dingshigang222@163.com

Received Sept. 8, 2017; Revision accepted Feb. 7, 2018; Crosschecked Sept. 11, 2018

Abstract: *Helicobacter pylori* infection is related to the development of gastric diseases. Our previous studies showed that high thioredoxin-1 (Trx1) expression in *H. pylori* can promote gastric carcinogenesis. To explore the underlying molecular mechanisms, we performed an isobaric tags for relative and absolute quantitation (iTRAQ)-based quantitative proteomic analysis of stomach tissues from Mongolian gerbil infected with *H. pylori* expressing high and low Trx1. Differences in the profiles of the expressed proteins were analyzed by bioinformatics and verified using Western blot analysis. We found three candidate proteins, 14-3-3α/β, glutathione-*S*-transferase (GST), and heat shock protein 70 (HSP70), in high Trx1 tissues compared with low Trx1 tissues and concluded that cellular stress and redox activity-related proteins were involved in the pathogenesis of gastric cancer associated with *H. pylori* Trx1.

Key words: Thioredoxin-1 (Trx1); *Helicobacter pylori*; Gastric carcinogenesis; Proteomics; Isobaric tags for relative and absolute quantitation (iTRAQ)
https://doi.org/10.1631/jzus.B1700456 **CLC number:** R573.9

1 Introduction

Gastric cancer is one of the most common cancers in the world. In China, incidence and mortality are high (Yang, 2006). *Helicobacter pylori* is thought to promote the pathogenesis of gastritis, peptic ulcer, and gastric cancer (Wroblewski et al., 2010). The discovery of *H. pylori* by Marshall and Warren (1984) was followed by many studies which indicated that *H. pylori* infection is associated with gastric carcinogenesis (Parsonnet et al., 1991; Blaser et al., 1995; Suerbaum and Michetti, 2002; Suriani et al., 2005). The International Agency for Research on Cancer classified *H. pylori* as a group I carcinogen (WHO, 1994). Long-term *H. pylori* colonization has also been shown to induce the development of gastric cancer in animals (Honda et al., 1998; Watanabe et al., 1998; Tsukamoto et al., 2013). However, the pathogenic mechanisms of *H. pylori* are still not clear.

‡ Corresponding author
* Project supported by the Key Laboratory for *Helicobacter pylori* Infection and Upper Gastrointestinal Diseases, Beijing Key Laboratory (No. BZ0371) and the National Natural Science Foundation of China (Nos. 81700496, 81270475, and 30770980)
# Electronic supplementary materials: The online version of this article (https://doi.org/10.1631/jzus.B1700456) contains supplementary materials, which are available to authorized users
ORCID: Yan-yan SHI, https://orcid.org/0000-0003-0247-371X; Shi-gang DING, https://orcid.org/0000-0002-0831-0965

Thioredoxin-1 (Trx1), encoded by HP0824 in *H. pylori* 26695, is one of several antioxidants in *H. pylori* (Baker et al., 2001). As an arginase chaperone, it mediates resistance to nitrosative and oxidative stresses, and is responsible for *H. pylori*'s ability to colonize and persist for decades in hostile gastric environments (Windle et al., 2000; Comtois et al., 2003; McGee et al., 2006; Wang et al., 2006; Kuhns et al., 2015). In previous studies, we found that Trx1 expression in *H. pylori* isolated from clinical gastric cancer tissues was significantly higher than that from gastritis tissues (Zhang et al., 2006), indicating that *H. pylori* Trx1 may be involved in the occurrence of gastric cancer. Further studies, both in vitro and in vivo, confirmed this finding (Shi et al., 2013; Liu et al., 2016). However, the mechanism by which *H. pylori* Trx1 has its carcinogenic effect is unknown.

We have explored the biological processes and molecular pathways through which *H. pylori* Trx1 exerts its pathogenic effects using proteomic technologies and Western blotting verification in Mongolian gerbils infected by *H. pylori* expressing either high or low Trx1, as described by Liu et al. (2016).

2 Materials and methods

2.1 Tissues of Mongolian gerbil models

All institutional and national guidelines for the care and use of laboratory animals were followed. After sacrifice, animal gastric tissues were taken for *H. pylori* culture and histological analysis and were snap-frozen in liquid nitrogen for protein extraction. Haematoxylin and eosin were used for histological analysis. Whilst establishing the gerbil model, we found that gastritis, dysplasia, and gastric cancer appeared gradually in the groups infected by *H. pylori* expressing high and low Trx1. We used tissues of varying degrees of gastric pathology for proteomic analysis, as follows: one control tissue (D23: 90 weeks without *H. pylori* infection), two chronic gastritis tissues (D4 and D22: 70 weeks after inoculation with *H. pylori* expressing high or low level of Trx1), two dysplasia tissues (C15 and C13: 90 weeks after *H. pylori* inoculation), and two gastric cancer tissues (C17 and C23: 90 weeks after *H. pylori* inoculation). Detailed information about the gerbils is provided in Table 1. We used seven more animals treated in the same way as above for Western blot analysis.

Table 1 Characteristics of individual gerbils

Animal number	Histopathologic diagnosis	Infection period (week)	*H. pylori* Trx1 level
D4	Gastritis	70	High
D22	Gastritis	70	Low
C15	Dysplasia	90	High
C13	Dysplasia	90	Low
C17	Gastric cancer	90	High
C23	Gastric cancer	90	Low
D23	Negative control	90	

2.2 Protein extraction

Gastric tissues were dissolved as described (Hsu et al., 2016) in lysis buffer (20 mmol/L Tris-HCl, 1 mmol/L ethylene diamine tetraacetic acid (EDTA), 1 mmol/L ethylene glycol tetraacetic acid (EGTA), 1% (v/v) Triton X-100, 50 mmol/L NaF, 20 mmol/L $Na_4P_2O_7$, 1 mmol/L Na_3VO_4, and protease inhibitors) and extracted with Precellys® homogenizer (Bertin Technologies, Saint Quentin en Yvelines Cedex, France). After homogenization, the tissue extracts were centrifuged at 14000 r/min for 20 min at 4 °C, and the supernatants were collected. A Bradford protein assay (Bio-Rad Laboratories, Inc., Hercules, CA, USA) was used to determine the protein concentrations; the protein samples were stored at −80 °C before use.

2.3 In-solution protein digestion, isobaric tags for relative and absolute quantitation (iTRAQ) labeling, and strong cationic-exchange (SCX) chromatography fractionation

Every protein sample (100 μg) was digested with Trypsin Gold (Promega, Madison, WI, USA) at 37 °C for 16 h. The peptides were then dried by vacuum centrifugation and reconstituted in 0.5 mol tetraethyl ammonium bromide (TEAB; Applied Biosystems, Milan, Italy). Groups of tissue extracts were labeled with different iTRAQ labeling reagents (C13: 114; C15: 115; C17: 116; C23: 117; D4: 118; D22: 119; D23: 121). The labeled samples were incubated for 2 h at room temperature, and then mixed and dried by vacuum centrifugation (Long et al., 2016).

High performance liquid chromatography (HPLC) Pump System (LC-20AB, Shimadzu, Kyoto, Japan) and Ultremex SCX column containing 5-μm particles (4.6 mm×250 mm, Phenomenex, USA) were coupled to SCX chromatography. The peptide mixtures were eluted for 15 min at a flow rate of 1 ml/min with 4 ml buffer A (10 mmol/L KH_2PO_4 in 25% (v/v) acetonitrile

(ACN), pH 3.0), and with a gradient of 0% (v/v) buffer B (10 mmol/L KH_2PO_4 and 2 mol/L KCl in 25% ACN, pH 3.0) for 30 min, 0–5% buffer B for 1 min, 5%–30% buffer B for 15 min, 30%–50% buffer B for 5 min, 50% buffer B for 5 min, 50%–100% buffer B for 5 min, and 100% buffer B for 10 min. The elution was monitored by absorbance at 214 nm, and fractions were collected every 1 min. Finally, the elution fractions were desalted with a Strata X C18 column (50 mm×2.1 mm, Phenomenex, USA), and the resultant fractions were vacuum-dried and re-suspended in buffer C (0.1% (v/v) formic acid) for further desalting.

2.4 Liquid chromatography-electrospray ionization-tandem mass spectrometry analysis

To analyze the iTRAQ-labeled peptide mixtures (Long et al., 2016), each fraction was reconstituted in buffer C, and then loaded onto nano-HPLC (LC-20AD, Shimadzu, Kyoto, Japan) by the autosampler onto a 2-cm C18 trap column, and separated on a resolving 10-cm analytical C18 column (inner diameter 75 μm). The samples were loaded at 8 μl/min for 5 min, and then the gradient was run at 400 nl/min starting from 5% (v/v) buffer D (ACN containing 0.1% (v/v) formic acid) for 10 min, 5%–30% buffer D for 30 min, 30%–60% buffer D for 5 min, 60%–80% buffer D for 3 min, 80% buffer D for 7 min, then returning to 5% buffer D in 3 min, and maintenance at 5% buffer D for 7 min.

A mass spectrometer (Q-Exactive, Thermo Fisher Scientific, San Jose, CA, USA) was coupled online to the HPLC. Peptides were detected by mass spectrometry (MS) analysis with a resolution of 70 000 and a mass range of 350–2000 m/z. The 15 most abundant precursor ions above a threshold ion count of 20 000 were selected for tandem MS (MS/MS) analysis. An electrospray voltage of 1.8 kV was applied. MS/MS analysis was recorded with a resolution of 17 500 and the mass range was automatically dependent on the range of MS analysis. Peptides were fractured with normalized collision energy of 27% and detected on the Q-Exactive.

2.5 Database search and protein quantification analysis

The MS/MS spectra were searched using the Mascot search engine (Version 2.3.02, Matrix Science, London, UK) against the SwissProt database containing rodentia protein sequences. The analysis allowed one missed cleavage from the trypsin digestion, and oxidation (M), Gln→Pyro-Glu (N-term Q), iTRAQ8plex (K), iTRAQ8plex (Y), and iTRAQ8plex (N-term) were set as the potential variable modifications, while carbamidomethyl (C) was set as fixed modifications. An automatic target-decoy search strategy was used in combination with percolator in order to score peptide spectral matches and so estimate the false discovery rate (FDR). Only peptides identified with strict spectral FDR of <1% (q-value< 0.01) were considered. The peptide precursor mass tolerance was 15×10^{-6} mg/L, MS/MS tolerance 20 mmu (millimass unit). Each confident protein identification was supported by at least one unique peptide. The quantitative protein ratios were weighted and normalized by the median ratio, the normalization method being median. Mascot software (Applied Biosystem, USA) was used to calculate the confidence of each quantitative protein based on the amount of spectrum. Modulated protein expression was defined as ≥1.2-fold change in expression level. Ratios with P-value of <0.05 were considered significantly different.

2.6 GO annotation, KEGG pathway enrichment, and network analysis

Proteins that had changed significantly were analyzed using the search tool DAVID (http://david.abcc.ncifcrf.gov) for gene ontology (GO) annotation and enrichment analysis, which includes three main modules: biological process, cellular component, and molecular function. The web-based Kyoto Encyclopedia of Genes and Genomes (KEGG, http://www.genome.p/kegg) was used for pathway analysis (Kanehisa et al., 2012). STRING (http://string.embl.de) was used as a database of predicted signaling networks and protein interactions (Deng et al., 2015).

2.7 Western blot analysis

Protein samples were analyzed by Western blot to validate the differentially expressed proteins. For protein extraction, tissues were ground and then suspended in lysis buffer containing a protease inhibitor mixture and shaken on ice for 30 min (Shi et al., 2013). The lysate was centrifuged at 15000g at 4 °C for 10 min, and the supernatant was collected.

The total protein concentration was measured by the Bradford method using a bicinchoninic acid (BCA) protein assay kit (Pierce, Rockford, IL, USA). Proteins (60 μg) were separated on 12% (0.12 g/ml) sodium dodecyl sulfate-polyacrylamide gel electrophoresis (SDS-PAGE) gels and electrophoretically transferred onto polyvinylidene fluoride (PVDF) membranes. The membranes were blocked in 5% (w/v) fat-free milk in Tris-buffered saline–0.5% (v/v) Tween-20 at room temperature for 1 h and incubated overnight at 4 °C with antibodies against heat shock protein 70 (HSP70, 1:500; Flarebio, China), glutathione-*S*-transferase (GST, 1:1000; Abcam, UK), 14-3-3α/β (1:500; BlueGene, China), and β-actin (1:2000; MBL, Japan). After three washes in phosphate-buffered saline (PBS) supplemented with 0.1% (v/v) Tween-20 for 15 min, the membranes were incubated with a secondary antibody, goat anti-rabbit IRDye 680 or goat anti-mouse IRDye 800CW (1:5000; LI-COR Biosciences, Lincoln, USA), for 1 h at room temperature. Proteins were identified by scanning the membranes using the Odyssey Imager System (LI-250A, LI-COR Biosciences, Lincoln, USA).

3 Results

3.1 Protein identification and quantification

We used an iTRAQ-based quantitative proteomic approach, as described above, to understand how the proteome changes in animal stomach tissues during the development of gastric cancer, and 792 differentially expressed proteins were identified from paired gastritis tissues infected with *H. pylori* expressing high or low Trx1, 677 proteins from paired dysplasia tissues, and 1116 proteins from paired gastric cancer tissues (Tables S1–S3). A total of 1506 different proteins were identified from the three groups, in which 242 proteins were common to all three groups. Fig. 1a is a Venn diagram showing the commonly and uniquely expressed proteins in the gastritis, dysplasia, and gastric cancer tissues.

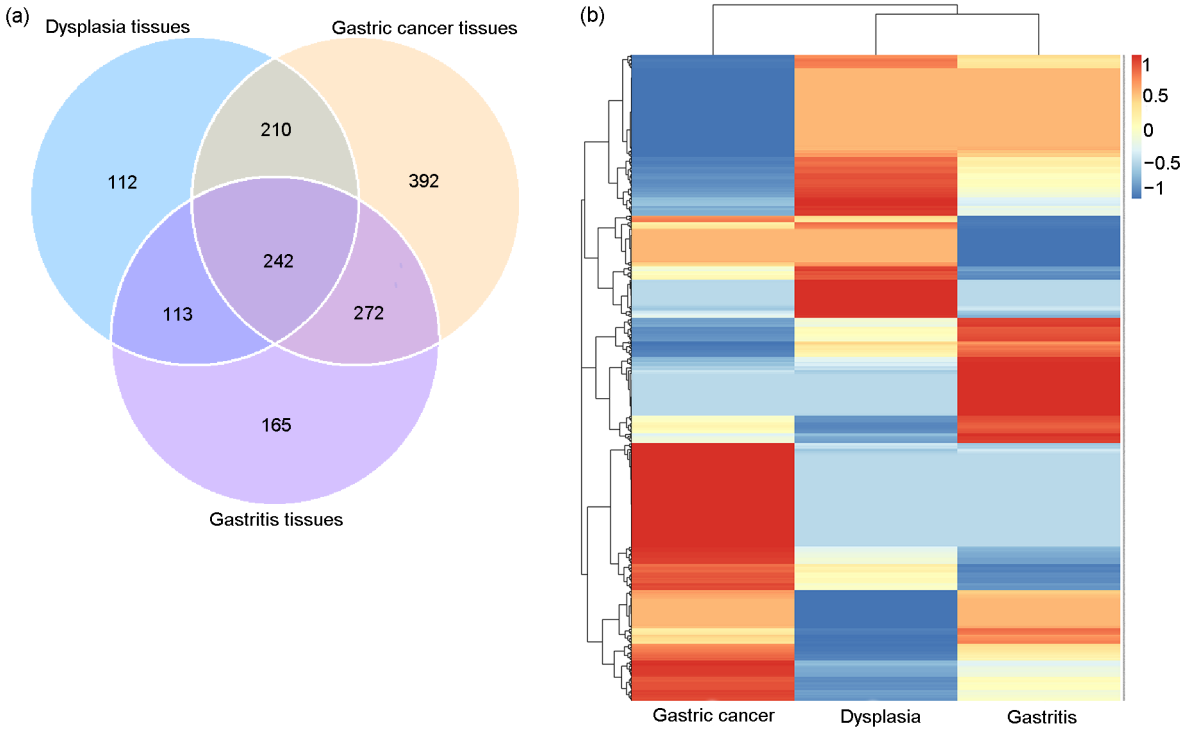

Fig. 1 Quantification and cluster analysis of the identified proteins

(a) Venn diagram showing the commonly and uniquely expressed 242 proteins in gastritis, dysplasia, and gastric cancer tissues infected by *H. pylori* expressing high or low thioredoxin-1 (Trx1). (b) Heatmap of the expression levels shown as $\log_2$ ratio of 1506 dysregulated proteins. The red-colored clusters represent up-regulated proteins and the blue-colored clusters represent down-regulated proteins (Note: for interpretation of the references to color in this figure legend, the reader is referred to the web version of this article)

3.2 Cluster analysis of the identified proteins

A heatmap was constructed from the data obtained for the differentially expressed proteins. Clustering analysis showed that the genes encoding these proteins are regulated (Fig. 1b, Table S4). 14-3-3α/β, HSP70, and GST were differentially expressed in all paired tissues (Table 2). These three proteins were also differentially expressed in the development of gastric cancer infected with *H. pylori* expressing high or low level of Trx1 (Table 3).

3.3 Functional classification and enrichment of *H. pylori* Trx1-regulated proteins

We classified the proteins identified in paired tissues infected with *H. pylori* expressing high or low Trx1, while results showed the same histopathological changes. Functional categories of the differentially expressed proteins are shown in Figs. 2–4.

For paired gastritis tissues D4 and D22, the top ten enriched GO terms within each major functional category are shown in Fig. 2. Figs. 2a–2c show the functional categories of proteins contributing the highest proportions. The top four most enriched GO terms under "biological process" included "protein localization", "homeostatic process", "cytoskeleton organization", and "intracellular transport" (Fig. 2a). The top ten categories of the differentially expressed proteins under "cellular component" are shown in Fig. 2b. "Intracellular non-membrane-bounded organelle" and "non-membrane-bounded organelle" had the most proteins, followed by "mitochondrion" and "cytoskeleton". In the molecular function category, "nucleotide binding", "purine nucleotide binding", and "cytoskeleton protein binding" were the most prominent categories (Fig. 2c). Fig. 2d shows the top ten functional categories of protein according to *P*-values of enriched GO terms.

For paired dysplasia tissues C15 and C13, the top four most enriched GO terms under "biological process" were "oxidation reduction", "cytoskeleton organization", "translation", and "macromolecular complex assembly" (Fig. 3a). The top ten categories of the differentially expressed proteins under "cellular component" are shown in Fig. 3b. For gastritis tissues, "intracellular non-membrane-bounded organelle" and "non-membrane-bounded organelle" had the most proteins, followed by "mitochondrion" and "cytoskeleton". In the molecular function category, "nucleotide binding", "calcium ion binding", and "structural molecule activity" were the most prominent categories (Fig. 3c). Fig. 3d shows the top ten functional categories of protein according to *P*-values of enriched GO terms.

For paired gastric cancer tissues C17 and C23, the top four most enriched GO terms under "biological process" included "oxidation reduction", "translation", "generation of precursor metabolites and energy", and "cytoskeleton organization" (Fig. 4a). The top ten categories of the differentially expressed proteins under "cellular component" are shown in Fig. 4b. As with gastritis tissues, "mitochondrion" and "organelle membrane" had the most proteins followed by "mitochondrial part". In the molecular function category, "nucleotide binding", "structural

Table 2 Expression ratios of candidate proteins in gastric tissues of Mongolian gerbils*

Disease	14-3-3α/β	HSP70	GST A2	GST A3	GST κ1
Gastritis	4.31	1.41	0.55	1.43	0.83
Dysplasia	1.79	0.71	1.47	0.43	0.82
Gastric cancer	2.82	0.66	0.34	0.64	1.25

* Ratio of the specific value of expression intensity of the protein in gastric tissues infected with *H. pylori* expressing high or low Trx1

Table 3 Expression ratios of candidate proteins in the development of gastric cancer infected with *H. pylori* expressing high or low Trx1*

Level of *H. pylori* Trx1	Disease	14-3-3α/β	HSP70	GST A2	GST A3	GST κ1
High	Negative control vs. gastritis	0.29	0.81	2.26	/	1.25
High	Gastritis vs. dysplasia	2.76	1.57	0.53	1.51	/
High	Dysplasia vs. gastric cancer	0.27	0.81	2.27	/	/
Low	Negative control vs. gastritis	3.18	/	1.21	1.33	/
Low	Gastritis vs. dysplasia	/	0.79	1.67	0.46	/
Low	Dysplasia vs. gastric cancer	0.51	0.77	0.51	1.33	1.60

* Ratio of the specific value of expression intensity of the protein in the development of gastric cancer infected with *H. pylori* expressing high or low Trx1. "/" represents no significant change

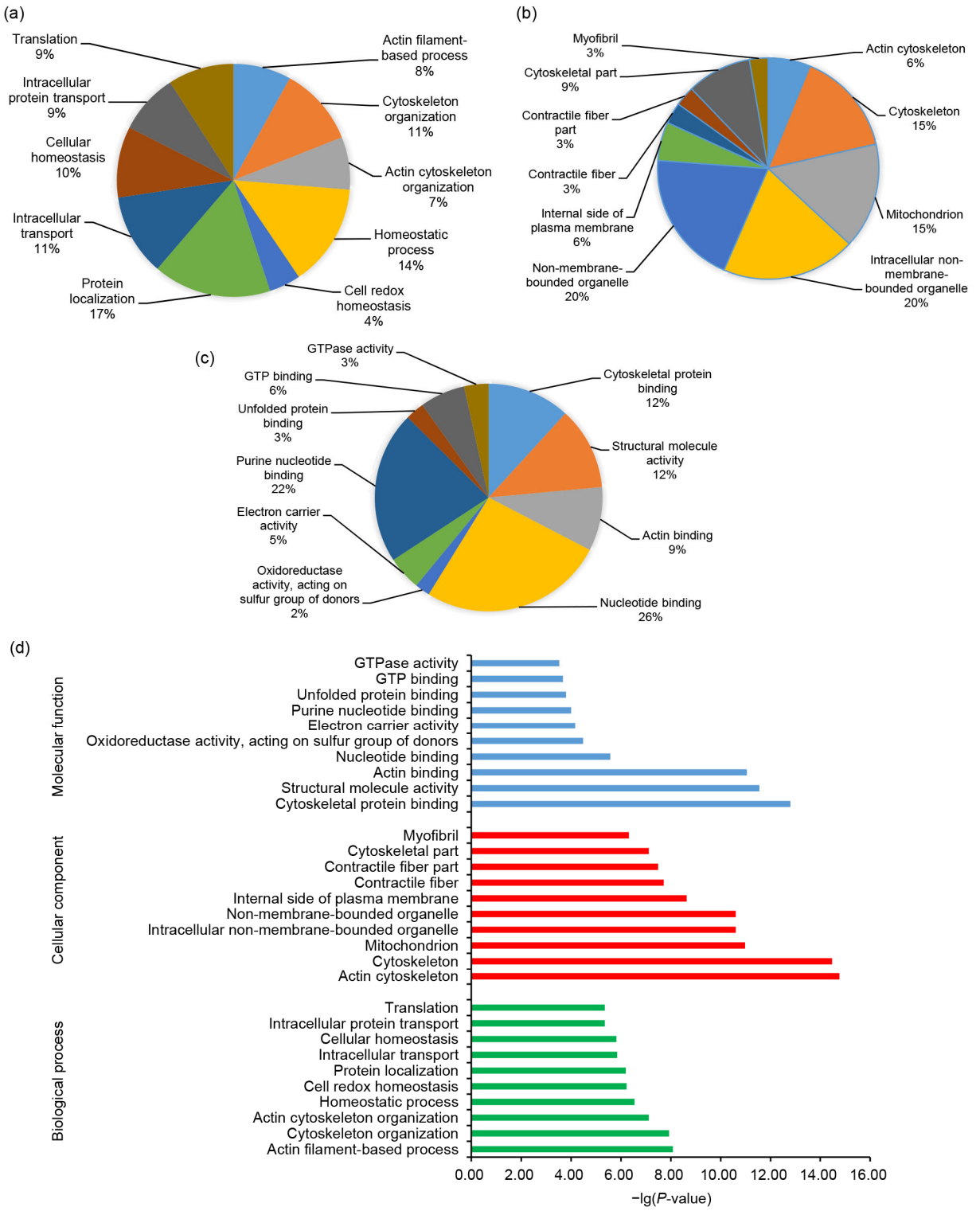

Fig. 2 GO annotation analysis of the differently expressed proteins for paired gastritis tissues infected by *H. pylori* expressing high or low Trx1

(a) Top ten enriched GO terms under "biological process". (b) Top ten enriched GO terms under "cellular component". (c) Top ten enriched GO terms under "molecular function". (d) Top ten functional categories of proteins according to *P*-values of enriched GO terms

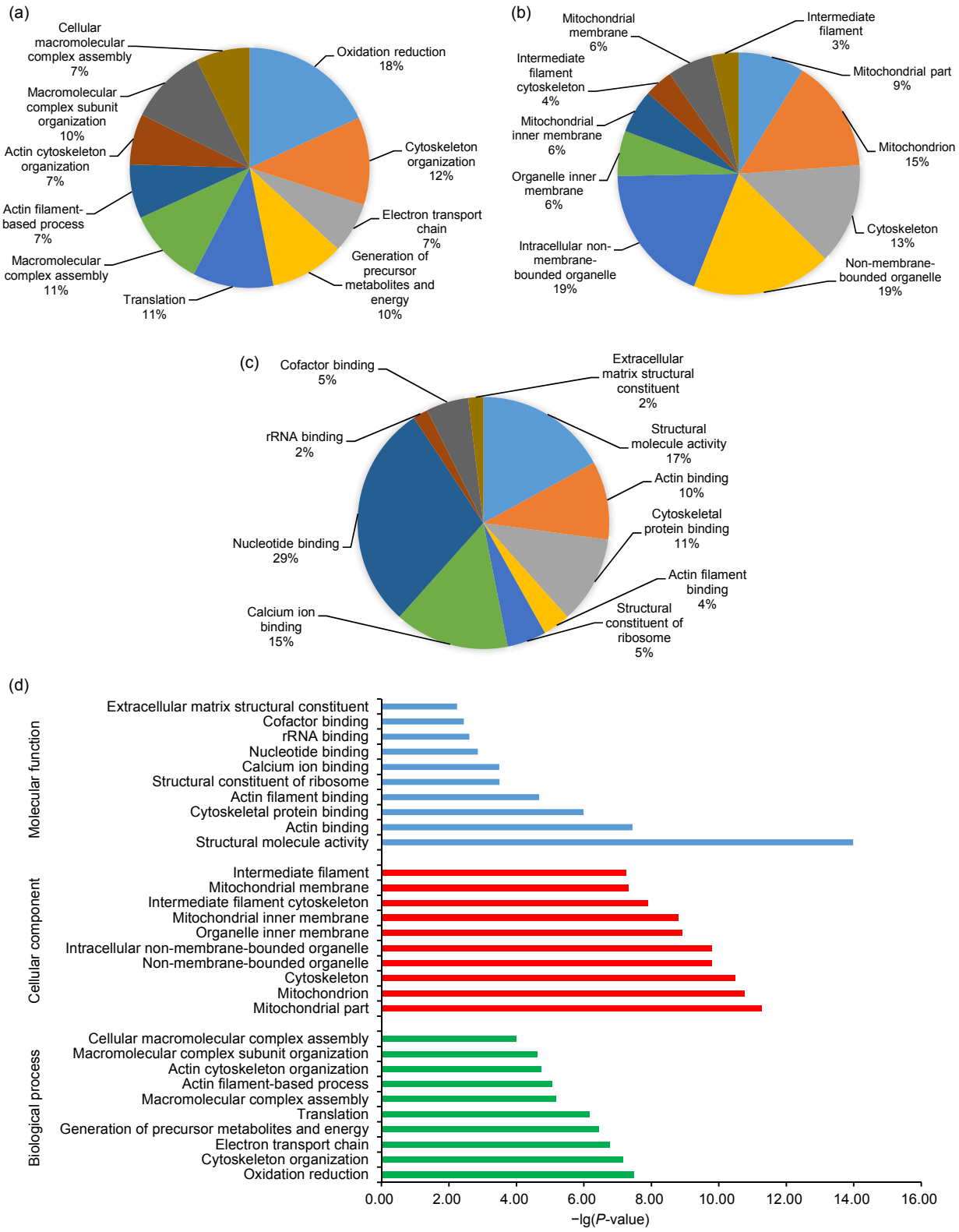

Fig. 3 GO annotation analysis of the differently expressed proteins for paired dysplasia tissues infected by *H. pylori* expressing high or low Trx1

(a) Top ten enriched GO terms under "biological process". (b) Top ten enriched GO terms under "cellular component". (c) Top ten enriched GO terms under "molecular function". (d) Top ten functional categories of proteins according to *P*-values of enriched GO terms

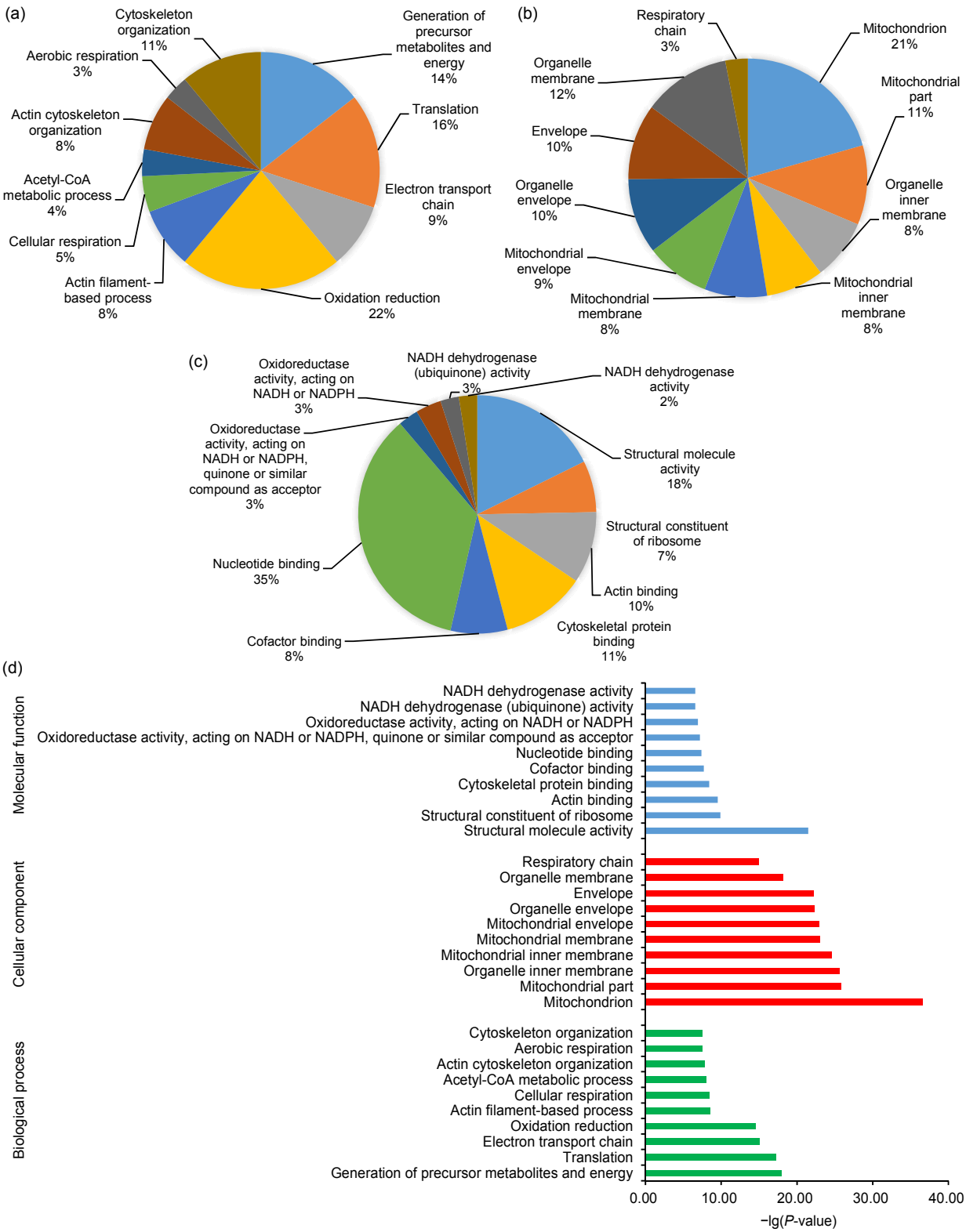

Fig. 4 GO annotation analysis of the differently expressed proteins for paired gastric cancer tissues infected by *H. pylori* expressing high or low Trx1

(a) Top ten enriched GO terms under "biological process". (b) Top ten enriched GO terms under "cellular component". (c) Top ten enriched GO terms under "molecular function". (d) Top ten functional categories of proteins according to *P*-values of enriched GO terms

molecule activity" and "cytoskeletal protein binding" were the most prominent categories (Fig. 4c). "Nucleotide binding" included 35% of identified proteins, which made it the most enriched GO term under the three major functional categories. Fig. 4d shows the top ten functional categories of protein according to *P*-values of enriched GO terms.

3.4 KEGG analysis of *H. pylori* Trx1-regulated proteins

The differentially expressed proteins were mapped to the KEGG database in order to identify the biological pathway operating during gastric carcinogenesis (Fig. 5). Among the 792 proteins identified in gastritis tissues D4 and D22, 410 proteins had KEGG orthology (KO) ID and were involved in 165 pathways. The top ten enriched pathways with *P*-values less than 0.05 are shown in Fig. 5a, and the top two were "focal adhesion" and "ECM-receptor interaction". Among the 677 proteins identified in dysplasia tissues C15 and C13, 350 proteins had KO ID and were involved in 170 pathways. The top ten enriched pathways with *P*-values less than 0.05 are shown in Fig. 5b, and the top two were "vascular smooth muscle contraction" and "systemic lupus erythematosus". Among the 1116 proteins identified in gastric cancer tissues C17 and C23, 624 proteins had KO ID and were involved in 188 pathways. The top ten enriched pathways with *P*-values less than 0.05 are shown in Fig. 5c, and the top two were "oxidative phosphorylation" and "Parkinson's disease".

3.5 Verification of three candidates

To support the results of proteomic analysis, we performed Western blot analysis to monitor changes in the three proteins implicated in gastric carcinogenesis, HSP70, GST, and 14-3-3α/β (Figs. 6a and 6b). The changes in HSP70 expression were found to be consistent with the proteome data. For GST, the changes in expression were found to be approximately consistent with the proteome data for gastritis and gastric cancer tissues. For 14-3-3α/β, the expression changes were consistent for all three kinds of tissue, while the fold change ratios in the high Trx1 group compared with low Trx1 group were less than one, indicating that these were not consistent with the proteome data (Fig. 6c).

4 Discussion

H. pylori is one of the pathogens involved in gastric carcinogenesis, which is a multifactorial and multistage process (Zheng et al., 2004). Half of the world's population is infected with *H. pylori*, but only a subpopulation develops severe digestive diseases (Suerbaum and Michetti, 2002; Abadi and Kusters, 2016). Studies of bacterial virulence factors will provide mechanistic evidence on gastric carcinogenesis and identify populations with a high risk of *H. pylori* infection. Many biomarkers have been considered to be critical to *H. pylori* virulence, such as cytotoxin-associated gene A (*cag*A) and vacuolating cytotoxin A (*vac*A) (Montecucco and Rappuoli, 2001; González et al., 2011). However, recently, it has been reported that other virulence factors may contribute significantly to the characteristics of *H. pylori* infection (Zhang et al., 2001; Fock et al., 2008): for example, the role of *cag*A has been reported to be

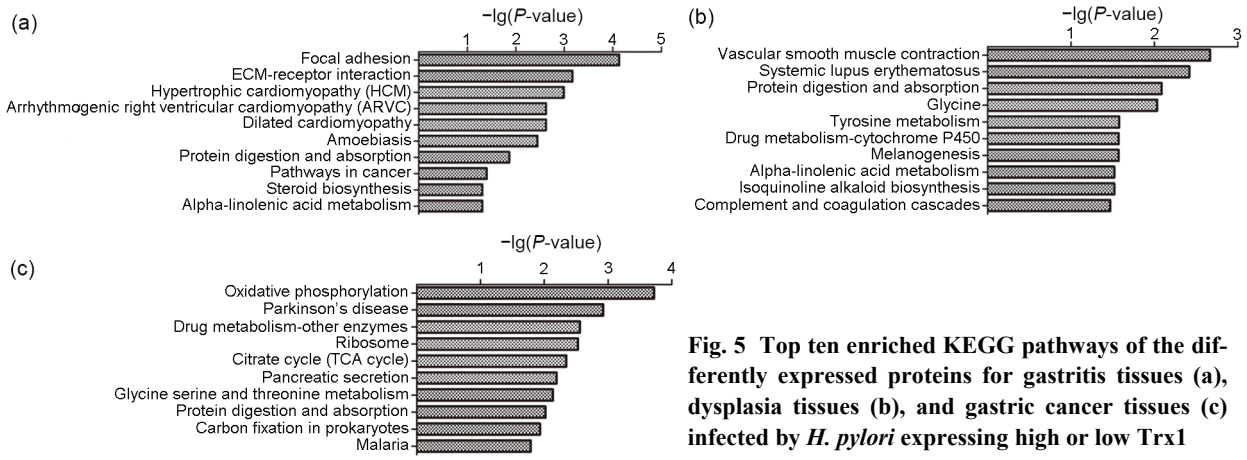

Fig. 5 Top ten enriched KEGG pathways of the differently expressed proteins for gastritis tissues (a), dysplasia tissues (b), and gastric cancer tissues (c) infected by *H. pylori* expressing high or low Trx1

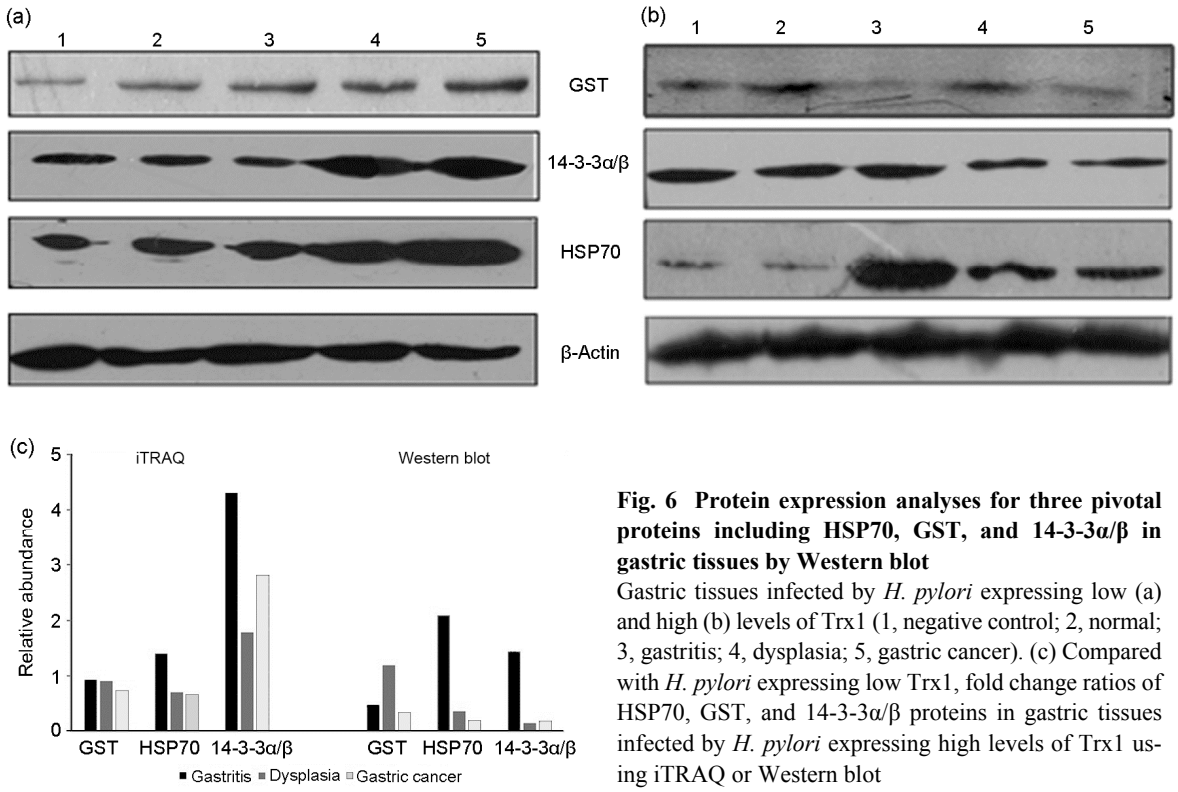

Fig. 6 Protein expression analyses for three pivotal proteins including HSP70, GST, and 14-3-3α/β in gastric tissues by Western blot

Gastric tissues infected by *H. pylori* expressing low (a) and high (b) levels of Trx1 (1, negative control; 2, normal; 3, gastritis; 4, dysplasia; 5, gastric cancer). (c) Compared with *H. pylori* expressing low Trx1, fold change ratios of HSP70, GST, and 14-3-3α/β proteins in gastric tissues infected by *H. pylori* expressing high levels of Trx1 using iTRAQ or Western blot

mediated by other factors (Wang et al., 2016). These other virulence factors require further research. Previous in vitro and in vivo studies found *H. pylori* Trx1 to be a potential virulence factor associated with gastric carcinogenesis with *H. pylori* expressing high levels of Trx1, which causes more serious tubular adenocarcinoma in a higher percentage of Mongolia gerbils compared with *H. pylori* expressing low Trx1 levels (Zhang et al., 2006; Shi et al., 2013; Liu et al., 2016). However, the mechanisms by which Trx1 promotes carcinogenesis are not clear.

In previous studies, we used *H. pylori* clinical isolates to infect gastric epithelial cells in vitro to determine that high Trx1 expression in *H. pylori* is associated with gastric carcinogenesis. The effects on cell lines were confirmed using the *H. pylori* Trx1-knockout mutant strain (Shi et al., 2013). For animal models, in our present study, we used clinical isolates to simulate real situations in clinical populations. Limited by the numbers of Mongolian gerbils, we did not use the *H. pylori* Trx1-knockout mutant strain, which was a limitation of this study (Liu et al., 2016).

We used an iTRAQ-based proteomic analysis to quantitatively profile the proteins of animal models infected by *H. pylori* and so revealed the central metabolic proteins in gastric carcinogenesis tissues, as well as gastritis, dysplasia, and gastric cancer tissues. The iTRAQ coupled with two dimensions (2D)-liquid chromatography (LC)-MS/MS analysis identified 1506 differentially expressed proteins. Expression of HSP70, GST, and 14-3-3α/β changed frequently in the developing stages of gastric carcinogenesis. Combined with the literature search, we focused on the three proteins thought to be associated with oxidative stress, cancer, and *H. pylori* infection.

GSTs are a family of detoxification enzymes which protect against the harmful effects of toxicants and carcinogens (Hayes et al., 2005). GSTs regulate the mitogen-activated protein (MAP) kinase pathway participating in cellular survival and death signals via interactions with c-Jun N-terminal kinase 1 (JNK1) and apoptosis signal-regulating kinase 1 (ASK1), which are activated in response to cellular stress. Cell apoptosis is inhibited and GST is therefore considered to be associated with tumorigenesis (Townsend and Tew, 2003). After *H. pylori* infection, GST can remove reactive oxygen species by the oxidation of the GST enzyme protein. Some studies have shown that GST expression is significantly up-regulated in *H.*

pylori-infected gastric mucosa (Baek et al., 2004). However, other studies reported that GST activity was significantly lower in *H. pylori*-positive gastric tissues than in *H. pylori*-negative tissues (Kim et al., 2005), implying that *H. pylori*-infection could antagonize the expression of GST, weakening its toxicant protection role and making it easier to damage the gastric mucosa barrier. Therefore, reduced GST activity may increase the risk of gastric cancers.

Compared with tissues infected with low Trx1 *H. pylori*, GST was down-regulated in tissues infected with high Trx1 *H. pylori*, especially in gastric cancer tissues. Research has shown that GST polymorphism and methylation may also be associated with *H. pylori*-infection or gastric carcinogenesis (García-González et al., 2012).

HSP70 which is abundant in all cellular compartments has a diverse array of cellular functions (Bellini et al., 2017; Cesa et al., 2017), including the refolding of misfolded or aggregated proteins (Cybulsky et al., 2016) and the facilitation of nuclear proteome stability upon thermal stress (Niforou et al., 2014). HSP70 expression can be induced by stresses such as oxidative stress and anticancer drugs and is at a very low level under normal conditions (Niforou et al., 2014). It plays important roles in cancer development, through anti-apoptotic effects and by inhibiting oncogene-induced senescence (Wu et al., 2017), and is often over-expressed in cancer cells. *H. pylori*-infection has been reported to inhibit the expression of HSP70 in gastric mucosa. Teprenone can restore HSP70 expression and inhibit inducible nitric oxide synthase (iNOS), implying that teprenone therapy can protect gastric mucosa cells from *H. pylori* infection (Yeo et al., 2004; Targosz et al., 2012). Other reports, however, show the opposite that HSP70 expression is progressively increased in gastric carcinogenesis (Carrasco et al., 2011). In our study, the fold change ratio of HSP70 expression in gastric mucosa infected by high and low Trx1 *H. pylori* infection was greater than one in gastritis, and was less than one in dysplasia and gastric cancer. Compared with low Trx1 *H. pylori*, HSP70 expression in gastritis tissues was up-regulated after infection with high Trx1 *H. pylori* and was down-regulated in dysplasia and gastric cancer tissues. This indicates that with high Trx1 *H. pylori* infection, the lower HSP70 in dysplasia and gastric cancer tissues makes it easier for *H. pylori* to damage gastric mucosa.

The 14-3-3 proteins are a family of conserved regulatory molecules, which are phospho-serine/threonine binding proteins that have important roles in the regulation of metabolism and signal transduction networks (Uhart and Bustos, 2014). 14-3-3 protein could bind Bcl-2-associated death promoter (BAD) and ASK1, which are known to induce apoptosis. Therefore 14-3-3 proteins may suppress apoptotic signaling. The expression of 14-3-3α/β isoform can be induced by oxidative stress by *H. pylori* infection associated with nuclear factor κB (NF-κB) activation in gastric epithelial cells (Lim et al., 2004; Zhou et al., 2017). In this study, we found that 14-3-3α/β is up-regulated by high Trx1 *H. pylori* infection in gastritis tissues. Previously, we suggested that expression of Trx1 as one of the antioxidant enzymes in *H. pylori* was related to reactive oxygen species (Shi et al., 2014). Further study should be performed on the specific role of *H. pylori* Trx1 and the α/β isoform of 14-3-3 protein on cell apoptosis and proliferation.

The protein profile in tissues from animal stomachs infected with *H. pylori* expressing high and low Trx1 revealed distinct patterns of proteins during *H. pylori* infection. *H. pylori* expressing a high level of Trx1 was associated with gastric carcinogenesis. Cellular stress and redox activity-related proteins, GST, HSP70, and 14-3-3α/β, were found to be involved in the pathogenesis of gastric cancer associated with *H. pylori*. Further exploration is needed into the mechanisms of action of these proteins, *H. pylori* Trx1, *H. pylori*-infection, and gastric carcinogenesis.

Acknowledgements

The authors thank Kai XIONG of Peking University (Beijing, China) for providing technological help.

Compliance with ethics guidelines

Yan-yan SHI, Jing ZHANG, Ting ZHANG, Man ZHOU, Ye WANG, He-jun ZHANG, and Shi-gang DING declare that they have no conflict of interest.

This article does not contain any studies with human or animal subjects performed by any one of the authors.

References

Abadi ATB, Kusters JG, 2016. Management of *Helicobacter pylori* infections. *BMC Gastroenterol*, 16:94.

https://doi.org/10.1186/s12876-016-0496-2

Baek HY, Lim JW, Kim H, et al., 2004. Oxidative-stress-related proteome changes in *Helicobacter pylori*-infected human gastric mucosa. *Biochem J*, 379(Pt 2):291-299. https://doi.org/10.1042/BJ20031208

Baker LMS, Raudonikiene A, Hoffman PS, et al., 2001. Essential thioredoxin-dependent peroxiredoxin system from *Helicobacter pylori*: genetic and kinetic characterization. *J Bacteriol*, 183(6):1961-1973. https://doi.org/10.1128/JB.183.6.1961-1973.2001

Bellini S, Barutta F, Mastrocola R, et al., 2017. Heat shock proteins in vascular diabetic complications: review and future perspective. *Int J Mol Sci*, 18(12):2709. https://doi.org/10.3390/ijms18122709

Blaser MJ, Chyou PH, Nomura A, 1995. Age at establishment of *Helicobacter pylori* infection and gastric carcinoma, gastric ulcer, and duodenal ulcer risk. *Cancer Res*, 55(3): 562-565.

Carrasco V, Canfrán S, Rodriguez-Franco F, et al., 2011. Canine gastric carcinoma: immunohistochemical expression of cell cycle proteins (p53, p21, and p16) and heat shock proteins (Hsp27 and Hsp70). *Vet Pathol*, 48(1): 322-329. https://doi.org/10.1177/0300985810375050

Cesa LC, Shao H, Srinivasan SR, et al., 2017. X-linked inhibitor of apoptosis protein (XIAP) is a client of heat shock protein 70 (Hsp70) and a biomarker of its inhibition. *J Biol Chem*, 293(7):2370-2380. https://doi.org/10.1074/jbc.RA117.000634

Comtois SL, Gidley MD, Kelly DJ, 2003. Role of the thioredoxin system and the thiol-peroxidases Tpx and Bcp in mediating resistance to oxidative and nitrosative stress in *Helicobacter pylori*. *Microbiology*, 149(Pt 1):121-129. https://doi.org/10.1099/mic.0.25896-0

Cybulsky AV, Guillemette J, Papillon J, 2016. Ste20-like kinase, SLK, activates the heat shock factor 1-Hsp70 pathway. *Biochim Biophys Acta*, 1863(9):2147-2155. https://doi.org/10.1016/j.bbamcr.2016.05.015

Deng W, Yan M, Yu T, et al., 2015. Quantitative proteomic analysis of the metastasis-inhibitory mechanism of miR-193a-3p in non-small cell lung cancer. *Cell Physiol Biochem*, 35(5):1677-1688. https://doi.org/10.1159/000373981

Fock KM, Talley N, Moayyedi P, et al., 2008. Asia-pacific consensus guidelines on gastric cancer prevention. *J Gastroenterol Hepatol*, 23(3):351-365. https://doi.org/10.1111/j.1440-1746.2008.05314.x

García-González MA, Quintero E, Bujanda L, et al., 2012. Relevance of *GSTM1*, *GSTT1*, and *GSTP1* gene polymorphisms to gastric cancer susceptibility and phenotype. *Mutagenesis*, 27(6):771-777. https://doi.org/10.1093/mutage/ges049

González CA, Figueiredo C, Lic CB, et al., 2011. *Helicobacter pylori cag*A and *vac*A genotypes as predictors of progression of gastric preneoplastic lesions: a long-term follow-up in a high-risk area in Spain. *Am J Gastroenterol*, 106(5):867-874. https://doi.org/10.1038/ajg.2011.1

Hayes JD, Flanagan JU, Jowsey IR, 2005. Glutathione transferases. *Annu Rev Pharmacol Toxicol*, 45:51-88. https://doi.org/10.1146/annurev.pharmtox.45.120403.095857

Honda S, Fujioka T, Tokieda M, et al., 1998. Development of *Helicobacter pylori*-induced gastric carcinoma in Mongolian gerbils. *Cancer Res*, 58(19):4255-4259.

Hsu CH, Hsu CW, Hsueh C, et al., 2016. Identification and characterization of potential biomarkers by quantitative tissue proteomics of primary lung adenocarcinoma. *Mol Cell Proteomics*, 15(7):2396-2410. https://doi.org/10.1074/mcp.M115.057026

Kanehisa M, Goto S, Sato Y, et al., 2012. KEGG for integration and interpretation of large-scale molecular data sets. *Nucleic Acids Res*, 40(D1):D109-D114. https://doi.org/10.1093/nar/gkr988

Kim HS, Kwack SJ, Lee BM, 2005. Alteration of cytochrome p-450 and glutathione *S*-transferase activity in normal and malignant human stomach. *J Toxicol Environ Health, Part A*, 68(19):1611-1620. https://doi.org/10.1080/15287390500182867

Kuhns LG, Wang G, Maier RJ, 2015. Comparative roles of the two *Helicobacter pylori* thioredoxins in preventing macromolecule damage. *Infect Immun*, 83(7):2935-2943. https://doi.org/10.1128/IAI.00232-15

Lim JW, Kim H, Kim JM, et al., 2004. Cellular stress-related protein expression in *Helicobacter pylori*-infected gastric epithelial AGS cells. *Int J Biochem Cell Biol*, 36(8): 1624-1634. https://doi.org/10.1016/j.biocel.2004.01.018

Liu LN, Ding SG, Shi YY, et al., 2016. *Helicobacter pylori* with high thioredoxin-1 expression promotes stomach carcinogenesis in Mongolian gerbils. *Clin Res Hepatol Gastroenterol*, 40(4):480-486. https://doi.org/10.1016/j.clinre.2015.11.001

Long BS, Muhamad R, Yan GK, et al., 2016. Quantitative proteomics analysis reveals glutamine deprivation activates fatty acid β-oxidation pathway in HepG2 cells. *Amino Acids*, 48(5):1297-1307. https://doi.org/10.1007/s00726-016-2182-7

Marshall BJ, Warren JR, 1984. Unidentified curved bacilli in the stomach of patients with gastritis and peptic ulceration. *Lancet*, 323(8390):1311-1315. https://doi.org/10.1016/S0140-6736(84)91816-6

McGee DJ, Kumar S, Viator RJ, et al., 2006. *Helicobacter pylori* thioredoxin is an arginase chaperone and guardian against oxidative and nitrosative stresses. *J Biol Chem*, 281(6):3290-3296. https://doi.org/10.1074/jbc.M506139200

Montecucco C, Rappuoli R, 2001. Living dangerously: how *Helicobacter pylori* survives in the human stomach. *Nat Rev Mol Cell Biol*, 2(6):457-466.

https://doi.org/10.1038/35073084

Niforou K, Cheimonidou C, Trougakos IP, 2014. Molecular chaperones and proteostasis regulation during redox imbalance. *Redox Biol*, 2:323-332. https://doi.org/10.1016/j.redox.2014.01.017

Parsonnet J, Friedman GD, Vandersteen DP, et al., 1991. *Helicobacter pylori* infection and the risk of gastric carcinoma. *N Engl J Med*, 325(16):1127-1131. https://doi.org/10.1056/nejm199110173251603

Shi YY, Liu LN, Zhang T, et al., 2013. The involvement of *Helicobacter pylori* thioredoxin-1 in gastric carcinogenesis. *J Med Microbiol*, 62(Pt 8):1226-1234. https://doi.org/10.1099/jmm.0.056903-0

Shi YY, Chen M, Zhang YX, et al., 2014. Expression of three essential antioxidants of *Helicobacter pylori* in clinical isolates. *J Zhejiang Univ-Sci B (Biomed & Biotechnol)*, 15(5):500-506. https://doi.org/10.1631/jzus.B1300171

Suerbaum S, Michetti P, 2002. *Helicobacter pylori* infection. *N Engl J Med*, 347(15):1175-1186. https://doi.org/10.1056/NEJMra020542

Suriani R, Venturini I, Taraglio S, et al., 2005. Type III intestinal metaplasia, *Helicobacter pylori* infection and gastric carcinoma risk index in an Italian series of 1750 patients. *Hepatogastroenterology*, 52(61):285-288.

Targosz A, Brzozowski T, Pierzchalski P, et al., 2012. *Helicobacter pylori* promotes apoptosis, activates cyclooxygenase (COX)-2 and inhibits heat shock protein HSP70 in gastric cancer epithelial cells. *Inflamm Res*, 61(9):955-966. https://doi.org/10.1007/s00011-012-0487-x

Townsend DM, Tew KD, 2003. The role of glutathione-*S*-transferase in anti-cancer drug resistance. *Oncogene*, 22(47):7369-7375. https://doi.org/10.1038/sj.onc.1206940

Tsukamoto T, Toyoda T, Mizoshita T, et al., 2013. *Helicobacter pylori* infection and gastric carcinogenesis in rodent models. *Semin Immunopathol*, 35(2):177-190. https://doi.org/10.1007/s00281-012-0357-1

Uhart M, Bustos DM, 2014. Protein intrinsic disorder and network connectivity. The case of 14-3-3 proteins. *Front Genet*, 5:10. https://doi.org/10.3389/fgene.2014.00010

Wang G, Alamuri P, Maier RJ, 2006. The diverse antioxidant systems of *Helicobacter pylori*. *Mol Microbiol*, 61(4):847-860. https://doi.org/10.1111/j.1365-2958.2006.05302.x

Wang G, Romero-Gallo J, Benoit SL, et al., 2016. Hydrogen metabolism in *Helicobacter pylori* plays a role in gastric carcinogenesis through facilitating CagA translocation. *mBio*, 7(4):e01022-16. https://doi.org/10.1128/mBio.01022-16

Watanabe T, Tada M, Nagai H, et al., 1998. *Helicobacter pylori* infection induces gastric cancer in Mongolian gerbils. *Gastroenterology*, 115(3):642-648. https://doi.org/10.1016/S0016-5085(98)70143-X

WHO, 1994. Schistosomes, Liver Flukes and *Helicobacter Pylori*. IARC Working Group on the Evaluation of Carcinogenic Risks to Humans. IARC Monographs on the Evaluation of Carcinogenic Risks to Humans, IARC Scientific Publication No. 61, IARC, Lyon, France.

Windle HJ, Fox Á, NíEidhin D, et al., 2000. The thioredoxin system of *Helicobacter pylori*. *J Biol Chem*, 275(7):5081-5089. https://doi.org/10.1074/jbc.275.7.5081

Wroblewski LE, Peek RM Jr, Wilson KT, 2010. *Helicobacter pylori* and gastric cancer: factors that modulate disease risk. *Clin Microbiol Rev*, 23(4):713-739. https://doi.org/10.1128/cmr.00011-10

Wu JM, Liu TE, Rios Z, et al., 2017. Heat shock proteins and cancer. *Trends Pharmacol Sci*, 38(3):226-256. https://doi.org/10.1016/j.tips.2016.11.009

Yang L, 2006. Incidence and mortality of gastric cancer in china. *World J Gastroenterol*, 12(1):17-20. https://doi.org/10.3748/wjg.v12.i1.17

Yeo M, Park HK, Kim DK, et al., 2004. Restoration of heat shock protein70 suppresses gastric mucosal inducible nitric oxide synthase expression induced by *Helicobacter pylori*. *Proteomics*, 4(11):3335-3342. https://doi.org/10.1002/pmic.200400951

Zhang J, Ding SG, Zhong LJ, et al., 2006. Difference analysis on proteome of *Helicobacter pylori* in patients with peptic ulcer, gastritis, and gastric cancer. *Nat Med J China*, 86(38):2690-2694 (in Chinese). https://doi.org/10.3760/j:issn:0376-2491.2006.38.007

Zhang YL, Liu HY, Zhou K, 2001. Lack of correlation of *vac*A genotype, *cag*A gene of *Helicobacter pylori* and their expression products with various gastroduodenal diseases. *Chin Med J (Engl)*, 114(7):703-706. https://doi.org/10.3760/j.issn:0366-6999.2001.07.008

Zheng Q, Chen XY, Shi Y, et al., 2004. Development of gastric adenocarcinoma in Mongolian gerbils after long-term infection with *Helicobacter pylori*. *J Gastroenterol Hepatol*, 19(10):1192-1198. https://doi.org/10.1111/j.1440-1746.2004.03469.x

Zhou XY, Hu DX, Chen RQ, et al., 2017. 14-3-3 Isoforms differentially regulate NFκB signaling in the brain after ischemia-reperfusion. *Neurochem Res*, 42(8):2354-2362. https://doi.org/10.1007/s11064-017-2255-3

List of electronic supplementary materials

Table S1 Different expressed proteins for paired gastritis tissues infected by *H. pylori* expressing high or low Trx1

Table S2 Different expressed proteins for paired dysplasia tissues infected by *H. pylori* expressing high or low Trx1

Table S3 Different expressed proteins for paired gastric cancer tissues infected by *H. pylori* expressing high or low Trx1

Table S4 Commonly and uniquely expressed 242 proteins in gastritis, dysplasia, and gastric cancer tissues infected by *H. pylori* expressing high or low Trx1

中文概要

题　目：细胞应激和氧化还原活性蛋白参与硫氧还蛋白-1高表达幽门螺杆菌感染所致胃黏膜的癌变

目　的：探索高表达硫氧还蛋白-1（Trx1）的幽门螺杆菌在致胃黏膜癌变过程中的作用机制。

创新点：首次分析临床分离菌株感染蒙古沙土鼠的胃黏膜疾病动物模型，首次对不同菌株感染所致的胃黏膜癌变相关分子机制进行探索。

方　法：用同位素标记相对和绝对定量（iTRAQ）蛋白质组学及生物信息学分析方法进行分析，并用免疫印迹法（Western blot）对重要分子进行验证。

结　论：高表达 Trx1 的幽门螺杆菌在致胃黏膜癌变过程中，三个重要的细胞应激和氧化还原活性蛋白包括 14-3-3α/β、谷胱甘肽转移酶（GST）和热休克蛋白（HSP70）参与致病。

关键词：硫氧还蛋白-1（Trx1）；幽门螺杆菌；胃黏膜癌变；蛋白质组学；同位素标记相对和绝对定量（iTRAQ）